INTERNATIONAL JOURNAL OF COMPUTERS COMMUNICATIONS & CONTROL
Online ISSN 1841-9844, ISSN-L 1841-9836, Volume: 21, Issue: 3, Month: June, Year: 2026
Article Number: 7444, https://doi.org/10.15837/ijccc.2026.3.7444

Design and Implementation of a PID-Controlled CC-CV Fast Charger for $LiFePO_4$ Batteries in Light Electric Vehicles

R. Syam, W. Djatmiko, I. Sugihartono, C. N. Trilia

Rafiuddin Syam
Department of Automation Engineering Technology
Faculty of Engineering, Universitas Negeri Jakarta, Indonesia
Corresponding author: rafiuddin_syam@unj.ac.id

Wisnu Djatmiko , and Cindy Novita Trilia
Department of Engineering Electronics Education
Faculty of Engineering, Universitas Negeri Jakarta, Indonesia
wisnu.dj@unj.ac.id and cindy.dantjie@gmail.com

Iwan Sugihartono
Department of Physics
Faculty of Science and Mathematics
Universitas Negeri Jakarta, Jakarta, Indonesia
iwan-sugihartono@unj.ac.id

Abstract

The widespread adoption of light electric vehicles (LEVs) is constrained by excessively long battery charging times, which reduce user convenience and practicality. This paper presents the design, implementation, and experimental validation of a PID-controlled constant current-constant voltage (CC-CV) fast-charging system tailored for a 12V, 6Ah lithium iron phosphate ($LiFePO_4$) battery, a typical energy storage unit in LEVs. The system integrates a buck converter for power regulation, an Arduino Uno microcontroller executing a parallel PID algorithm, and real-time feedback from voltage and current sensors. Charging tests were conducted from 90% depth of discharge (12V) using three protocols: conventional constant voltage (CV), CC-CV at 0.5C (3A), and CC-CV at 1C (6A). The PID-controlled CC-CV method drastically reduced charging time, achieving full charge in 2 hours and 1 minute at 0.5C (78.8% reduction) and 1h7min at 1C (88.2% reduction) compared to 9h 33min for CV charging. The dynamic behavior during the constant-voltage phase was further analyzed via closed-loop transfer function modeling. Using a first-order plus dead time (FOPTD) plant identified from step response data ($\tau = 39$ s, $L = 9$ s) and PID parameters ($K_p = 0.3$, $K_i = 0.02$, $K_d = 0.05$), the step response exhibits a rise time of 43.7 s, settling time of 151.3 s, and overshoot of 14.7%. Closed-loop poles at -0.2078 and $-0.0142 \pm j0.0342$ confirm stability and predict a lightly damped oscillatory mode consistent with experimental observations. The consistency between experimental and simulated responses validates the modeling approach and controller tuning. This research provides a validated framework for low-cost, embedded fast-charging solutions, contributing to the acceleration of LEV adoption and sustainable urban mobility.

Keywords: Battery management system, CC-CV method, fast charging, $LiFePO_4$ battery, light electric vehicle, PID control.

1 Introduction

The rapid proliferation of light electric vehicles (LEVs), including electric scooters, bicycles, and motorcycles, has emerged as a transformative solution for urban mobility challenges in densely populated developing nations. These vehicles offer affordable, agile, and environmentally sustainable transportation alternatives that alleviate traffic congestion and reduce urban air pollution [1]. However, despite their growing popularity, the widespread adoption of LEVs remains constrained by a critical technological limitation: excessively prolonged battery charging times[2]. Unlike conventional internal combustion engine vehicles that can be refueled in minutes, LEV batteries typically require several hours to reach full capacity, creating significant inconvenience for users and limiting vehicle utility for daily transportation needs. This range and time inconvenience constitute primary deterrents for potential adopters, undermining the environmental and social benefits that LEV proliferation could otherwise deliver. The urgency of addressing this challenge is particularly acute in urban centers where LEVs serve as primary mobility tools for millions of commuters, and where extended charging durations directly impact productivity and quality of life.

The fundamental technical problem lies in the limitations of conventional battery charging methodologies. Traditional constant voltage (CV) charging, while simple to implement, suffers from inherent inefficiency due to unregulated current profiles that produce high initial currents followed by prolonged exponential decay phases. The constant current-constant voltage (CC-CV) method has been established as a superior alternative, offering controlled two-stage charging that first delivers constant current until a voltage threshold is reached, then maintains constant voltage while current naturally decays [6, 7, 11]. However, implementing effective CC-CV charging requires sophisticated control systems that can dynamically regulate power electronics while responding to real-time battery conditions. Lithium iron phosphate ($LiFePO_4$) batteries, which dominate the LEV market due to their superior safety profile, long cycle life, and stable voltage characteristics, present specific charging requirements that demand precise control strategies [9, 10, 11]. The core technical challenge, therefore, is to develop a control system capable of maintaining precise current and voltage regulation throughout the charging process while adapting to the varying dynamics of the battery-converter system.

Despite significant research efforts in battery charging technologies, a notable research gap persists in the literature. Comparative analyses of $LiFePO_4$ and conventional Li-ion batteries have confirmed the superior capacity and efficiency of $LiFePO_4$ chemistry while documenting charging durations of approximately 90 minutes at 0.68C [12, 13, 14]. Additional studies have examined the relationship between voltage and state of charge [17], proposed refined constant voltage methods for capacity optimization [18], and investigated degradation mechanisms associated with high-rate charging [19, 20, 21, 22]. Recent advancements in multi-stage constant current charging [23] and adaptive CC-CV strategies based on open-circuit voltage estimation [24] have demonstrated the potential for optimized charging protocols. However, no study has comprehensively implemented and validated PID-controlled CC-CV fast charging specifically for complete 12V $LiFePO_4$ battery packs with systematic variation of C-rates (0.5C and 1C) under realistic operating conditions, while simultaneously providing analytical modeling of closed-loop dynamics and experimental validation of controller performance.

Recent advancements in fast-charging strategies have introduced sophisticated approaches to optimize charging speed while preserving battery health. Multi-stage constant current (MSCC) charging [23] employs multiple current steps tailored to the battery's state of charge, achieving reduced charging times through optimized current profiles. Similarly, adaptive CC-CV methods based on real-time state-of-charge estimation [24] dynamically adjust transition thresholds to accommodate battery aging and temperature variations. While these advanced algorithms demonstrate promising results, they often require complex optimization routines, accurate battery models, or additional sensors, which can increase implementation complexity and cost. Consequently, a notable research gap persists in the literature: a validated, low-cost fast-charging solution that couples rigorous closed-loop control analysis with practical hardware implementation for light electric vehicles (LEVs) remains underrepresented. Most existing studies focus either on theoretical control development without experimental validation on complete battery packs, or on hardware prototypes lacking analytical characterization of system dynamics and stability. This study addresses this gap by presenting a PID-controlled CC-CV charger that combines systematic modeling, closed-loop analysis, and experimental validation on a 12V 6Ah

$LiFePO_4$ battery pack, all realized using low-cost, commercially available components suitable for widespread adoption in emerging economies.

The novelty lies in the integration of rigorous closed-loop dynamic analysis with a low-cost embedded implementation, validated across multiple C-rates—a combination not previously reported for complete 12V 6Ah LiFePO4 battery packs. This study makes three distinct contributions that address the identified research gap. First, it presents a complete hardware implementation of a PID-controlled CC-CV fast charger for a 12V 6Ah LiFePO4 battery pack, integrating a buck converter, Arduino-based control, and real-time feedback using low-cost, commercially available components, such as the Arduino Uno, ACS712 sensor, and LM2596 buck converter. Second, it provides comprehensive analytical modeling of the closed-loop system dynamics using first-order plus dead time (FOPDT) identification and Padé approximation, with detailed analysis of step response characteristics and closed-loop pole locations that confirm system stability. Third, Systematic experimental validation is performed across three distinct charging protocols—conventional CV, CC-CV at 0.5C, and CC-CV at 1C — with repeatability assessment, yielding empirical evidence of substantial charging time reductions alongside sustained precise regulation critical for battery longevity.

The primary objective of this study is to design, implement, and experimentally validate a PID-controlled CC-CV fast-charging system for a 12V 6Ah $LiFePO_4$ battery, a typical energy storage unit in light electric vehicles. This research aims to achieve charging time reductions of at least 75% compared to conventional CV charging while maintaining stable voltage and current regulation throughout the charging process. By bridging the gap between theoretical control design and low-cost embedded implementation, this work contributes to the democratization of fast-charging technology in emerging economies like Indonesia, aligning with national electric vehicle acceleration policies through Presidential Regulation No. 55/2019 [3, 4, 5] and providing a validated framework for accelerating LEV adoption in developing nations.

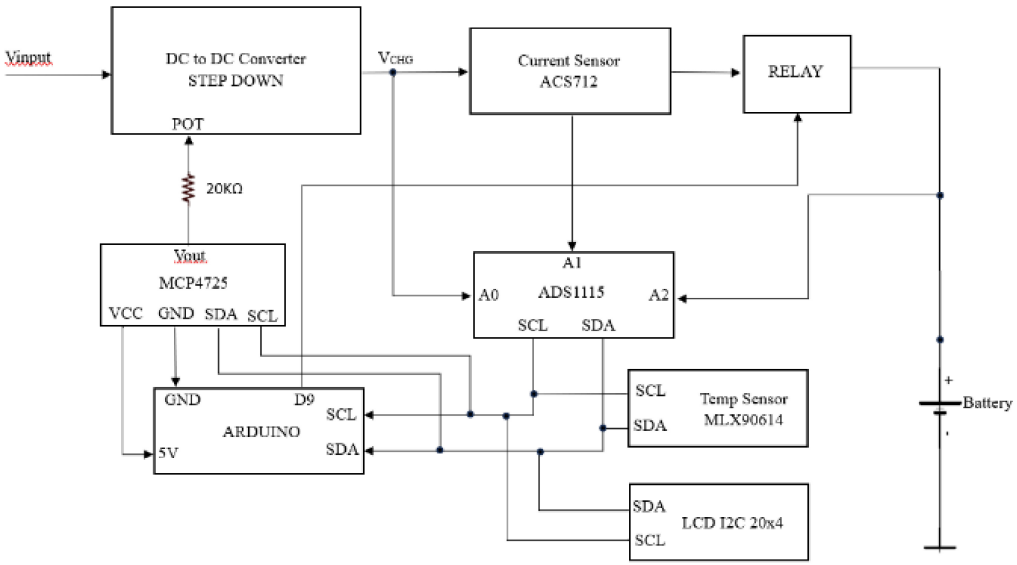

Figure 1: Circuit Layout Design

2 Theoretical Framework

2.1 The C-Rate Metric

The charging and discharging characteristics of a battery are fundamentally governed by the C-rate, a dimensionless parameter that quantifies the rate of current flow relative to the battery's nominal capacity (Ah). Defined as the charge or discharge current divided by the theoretical current required to fully deplete its rated capacity in one hour, the C-rate provides a standardized measure for comparing

performance across different battery sizes and chemistries [12, 13]. For instance, a C-rate of 1C for a 6Ah battery corresponds to a current of 6A, while 0.5C corresponds to 3A.

The C-rate is inversely proportional to the time required for a full charge or discharge cycle; a 1C rate implies an approximate completion time of one hour, whereas a 0.5C rate extends this duration to approximately two hours. It is critical to note that the effective capacity of a battery is not a static value but is intrinsically linked to the magnitude of the applied C-rate due to phenomena such as internal resistance and polarization losses, with higher C-rates often resulting in reduced utilizable capacity [19]. Therefore, the selection of an appropriate C-rate is essential for balancing charging speed with battery health and longevity.

2.2 Constant Current-Constant Voltage (CC-CV) Charging Method

The constant current-constant voltage (CC-CV) charging method is the predominant charging protocol for lithium-ion batteries, including $LiFePO_4$ chemistry, due to its ability to maximize charge acceptance while preventing overvoltage and overcurrent conditions [6, 7, 11]. The CC-CV method consists of two distinct phases:

1. **Constant Current (CC) Phase:** During this initial phase, the charger delivers a constant current to the battery while allowing the voltage to rise naturally. The current is typically set at a specific C-rate (e.g., 0.5C or 1C) based on the battery's specifications and desired charging speed. This phase continues until the battery voltage reaches a predefined threshold, which for $LiFePO_4$ batteries is typically 14.4V for a 12V nominal pack.

2. **Constant Voltage (CV) Phase:** Once the voltage threshold is reached, the charger switches to constant voltage mode, maintaining the voltage at the absorption level while allowing the charging current to decay exponentially. This phase continues until the current falls below a termination threshold (typically 0.06A or 1% of rated capacity), indicating that the battery has reached full state of charge.

The CC-CV method offers significant advantages over conventional constant voltage (CV) charging, which suffers from unregulated current profiles that produce high initial currents followed by prolonged exponential decay phases. By maintaining controlled current delivery during the CC phase and precise voltage regulation during the CV phase, the CC-CV method minimizes charging time while protecting the battery from overvoltage stress and internal polarization effects [26].

2.3 PID Control Fundamentals for Battery Charging

Proportional-Integral-Derivative (PID) control has emerged as a fundamental and widely adopted control strategy in battery charging applications due to its simplicity, effectiveness, and ability to maintain precise regulation of critical charging parameters [15]. In the context of battery charging, the primary objective of a PID controller is to regulate either the charging current during the CC phase or the charging voltage during the CV phase, ensuring that these parameters remain at their respective setpoints despite disturbances and nonlinearities inherent in the battery-converter system.

2.3.1 Continuous-Time PID Controller

The general form of a parallel PID controller in the continuous time domain is expressed as:

$$u(t) = K_p e(t) + K_i \int_0^t e(\tau)d\tau + K_d \frac{de(t)}{dt} \tag{1}$$

where $u(t)$ is the control signal (PWM duty cycle) applied to the buck converter, $e(t) = r(t) - y(t)$ is the error signal defined as the difference between the reference setpoint $r(t)$ (desired current or voltage) and the measured output $y(t)$ (actual current or voltage), K_p is the proportional gain which determines the immediate corrective action proportional to the current error, K_i is the integral gain which eliminates steady-state offset by accounting for the accumulation of past errors, and K_d is

the derivative gain which anticipates future error based on its rate of change, adding damping and improving transient response.

In the Laplace domain, the PID controller transfer function is represented as:

$$C(s) = \frac{U(s)}{E(s)} = K_p + \frac{K_i}{s} + K_d s = \frac{K_d s^2 + K_p s + K_i}{s} \tag{2}$$

2.3.2 PID Control Action in Battery Charging

The application of PID control to CC-CV charging protocols offers distinct advantages over conventional open-loop or hysteresis-based methods. During the constant current phase, the PID controller continuously adjusts the PWM duty cycle of the buck converter to maintain a constant current despite variations in battery voltage and load conditions. The proportional term provides immediate corrective action in response to current errors, ensuring rapid disturbance rejection. The integral term accumulates past errors, eliminating steady-state offset and guaranteeing precise current tracking. The derivative term anticipates future error, damping oscillations that might arise from sudden disturbances or changes in battery internal resistance, ensuring safe operation throughout the CC phase.

As the battery approaches the voltage threshold, the controller seamlessly transitions to the constant voltage phase, regulating the voltage at the absorption level while allowing current to decay naturally. The derivative action critically dampens oscillations arising from the interaction between converter switching dynamics and the battery's electrochemical response. The proportional term provides continuous corrective action to maintain the 14.4V setpoint, while the integral term ensures zero steady-state error despite parameter uncertainties. Lower gains compared to the CC phase reflect the need for conservative control to prevent overshoot and voltage excursions that could damage the battery.

The smooth transition between CC and CV phases is critical for preventing overvoltage stress and minimizing internal polarization effects that degrade battery health. The PID controller's gain adaptability ensures seamless transitions and stable operation throughout charging, with derivative action providing additional damping during transition. Integral anti-windup mechanisms prevent excessive error accumulation. The result combines speed with stability, delivering rapid charging times demanded by modern light electric vehicles while maintaining precision necessary to protect battery cycle life across varying chemistries, states of charge, and operating temperatures.

2.3.3 Discrete-Time PID Implementation and Practical Enhancements

In microcontroller-based implementations such as the Arduino Uno, the PID controller must be discretized for digital execution. A fixed sampling period of $T_s = 1\,\text{s}$ was selected based on the dominant dynamics of the battery charging process[16]. The thermal and electrochemical transients exhibit time constants on the order of tens of seconds, as evidenced by the identified plant time constant $\tau = 39\,\text{s}$. Hence, a sampling rate of 1 Hz is sufficient to capture the relevant dynamics without imposing excessive computational overhead on the low-cost embedded platform. The discrete-time PID algorithm follows the incremental (velocity) form to avoid integral windup and ensure smooth transitions:

$$\Delta u(k) = K_p[e(k) - e(k-1)] + K_i T_s e(k) + \frac{K_d}{T_s}[e(k) - 2e(k-1) + e(k-2)], \tag{3}$$

where k denotes the discrete time step and $e(k)$ is the error signal. The actual control signal is updated as $u(k) = u(k-1) + \Delta u(k)$, with the output $u(k)$ constrained to the permissible PWM duty cycle range [0, 255] to prevent actuator saturation.

To ensure reliable operation under real-world conditions, two practical enhancements were implemented. First, anti-windup protection is applied by clamping the integral term when the control output saturates. The integral accumulation is halted whenever $u(k)$ reaches its upper or lower limit and the error has the same sign as the saturated output, preventing excessive overshoot and instability. Second, a low-pass filter is incorporated into the derivative term to attenuate high-frequency noise from

the analog current and voltage sensors. Without filtering, the derivative action would amplify sensor noise, leading to erratic control behavior. The filtered derivative is implemented using a first-order low-pass filter with a cut-off frequency chosen to preserve the dominant dynamics while suppressing noise above approximately 0.5 Hz. These enhancements allow the theoretical PID performance to translate effectively into stable and precise control on the embedded hardware, as confirmed by the experimental results in Section 3.

2.4 PID Tuning for Battery Charging Systems

The tuning of PID parameters is a critical step in ensuring optimal performance of the charging system, as it directly influences the stability, responsiveness, and accuracy of current and voltage regulation. The objective of tuning is to determine the proportional (K_p), integral (K_i), and derivative (K_d) gains that minimize error while maintaining smooth control action and avoiding oscillations or overshoot.

2.4.1 Tuning Methodology

The tuning process employs a combination of model-based design and empirical refinement. First, the plant comprising the buck converter with battery load is characterized through step response experiments, yielding a first-order plus dead time (FOPTD) model with parameters time constant τ and dead time L. Subsequently, using the identified FOPTD model, initial PID gains are estimated via the Ziegler-Nichols tuning rules, which provide a systematic starting point based on the plant's transient response. Finally, fine-tuning is performed through iterative simulations and experimental validation to optimize performance under real operating conditions, with tuning criteria that include minimizing settling time, limiting overshoot, ensuring zero steady-state error, and maintaining smooth control action without excessive actuator saturation for the $LiFePO_4$ battery charging application.

2.4.2 Phase-Specific PID Parameters

Due to the inherently different dynamics and control objectives of each phase, PID parameters are tuned separately for the constant current (CC) and constant voltage (CV) phases. For the CC phase, where the controller maintains a fixed current setpoint at either 3A for 0.5C or 6A for 1C, higher proportional and derivative gains are employed to enable fast tracking of the current reference and rapid rejection of disturbances such as sudden changes in battery internal resistance. The proportional gain $K_p = 0.5$ provides immediate corrective action, while the derivative gain $K_d = 0.1$ improves transient response by damping oscillations. The integral gain $K_i = 0.05$ ensures elimination of steady-state error, guaranteeing that the actual charging current precisely matches the desired C-rate throughout the phase. These parameters provide a responsive yet stable control action, as evidenced by the smooth linear increase in battery voltage observed experimentally during the CC phase.

For the CV phase, where the controller regulates the voltage at 14.4V while allowing the current to decay naturally, more conservative control is required to prevent overshoot and voltage excursions that could damage the battery. The lower proportional gain $K_p = 0.3$ and integral gain $K_i = 0.02$ compared to the CC phase reflect this need for cautious regulation, while the derivative gain $K_d = 0.05$ adds critical damping to mitigate oscillations that might arise from the interaction between converter dynamics and the battery's electrochemical response. This parameter set ensures a smooth transition from the CC phase and maintains precise voltage regulation during the exponential current decay, with the integral term, though small, remaining essential for eliminating any residual voltage offset that could prevent the battery from reaching full capacity. Both experimental profiles and simulation results confirm the effectiveness of these phase-specific parameters.

2.4.3 Tuning Procedure

The tuning procedure for the PID controller was conducted in two stages: initial parameter estimation using the Ziegler-Nichols open-loop (reaction curve) method, followed by iterative fine-tuning through simulation and experimental validation to meet specific performance criteria.

The first step involved characterizing the plant dynamics, which consists of the buck converter and the $LiFePO_4$ battery load. A step change was applied to the PWM duty cycle, and the resulting output voltage response was recorded. The plant was identified as a first-order plus dead time (FOPTD) system, as described in Section 2.5.1 , with parameters static gain $K = 1$, time constant $\tau = 39\,\text{s}$, and dead time $L = 9\,\text{s}$. Using these values, the Ziegler-Nichols open-loop tuning rules for a PID controller provided the initial gains:

$$K_p = \frac{1.2 \cdot \tau}{K \cdot L} = 5.2, \quad K_i = \frac{K_p}{2L} = 0.289, \quad K_d = 0.5 \cdot K_p \cdot L = 23.4.$$

These initial gains produced an aggressive response characterized by excessive overshoot and oscillations, which is unsafe for battery charging applications. Therefore, a fine-tuning stage was performed using iterative simulations and experimental tests to refine the parameters. The fine-tuning process aimed to satisfy the following performance criteria, defined separately for each charging phase: During

Table 1: Performance criteria for PID tuning

Phase	**Performance Criteria**
Constant Current (CC)	Settling time $< 60\,\text{s}$, current overshoot $< 10\%$, zero steady-state error, and smooth PWM control without chattering.
Constant Voltage (CV)	Settling time $< 150\,\text{s}$, voltage overshoot $< 5\%$ (to remain below the battery's maximum rating of $14.6\,\text{V}$), zero steady-state error, and a well-damped transient response.

fine-tuning, the proportional and derivative gains were progressively reduced from the initial Ziegler-Nichols values to damp oscillations and avoid voltage overshoot, while the integral gain was adjusted to maintain zero steady-state error without causing integrator windup. Because the dynamics of the CC and CV phases differ significantly, separate parameter sets were tuned. The resulting parameters, presented in Section 2.4.2, were $K_p = 0.5$, $K_i = 0.05$, $K_d = 0.1$ for the CC phase and $K_p = 0.3$, $K_i = 0.02$, $K_d = 0.05$ for the CV phase. These final values were implemented in discrete form on the Arduino Uno microcontroller with a sampling period $T_s = 1\,\text{s}$, incorporating anti-windup protection and a low-pass filter on the derivative term to mitigate sensor noise. The effectiveness of the tuning procedure was validated through the experimental results presented in Section 3, confirming that the system meets the prescribed performance criteria while delivering substantial reductions in charging time.

2.5 System Modeling and Transfer Functions

To enable rigorous control design and stability analysis, the dynamic behavior of the charging system is mathematically modeled using system identification techniques[27]. The plant, comprising the buck converter and the $LiFePO_4$ battery load, is characterized through open-loop step response experiments following the Ziegler-Nichols method.

2.5.1 FOPTD Model and Identification Procedure

The dynamic behavior of the charging system was characterized through an open-loop step response test. The plant, comprising the buck converter and the $LiFePO_4$ battery load, was first brought to a known steady-state operating point: the battery was partially discharged to an open-circuit voltage of approximately $13.0\,\text{V}$, and the buck converter was driven with a constant PWM duty cycle that produced a steady output voltage of $13.0\,\text{V}$. A step change was then applied to the duty cycle, increasing it by a fixed increment corresponding to a voltage setpoint rise of about $1.5\,\text{V}$, and the resulting output voltage was recorded in real time using the Arduino Uno's analog-to-digital converter at a sampling rate of $1\,\text{s}$. From the recorded step response, the plant was identified as a first-order plus dead time (FOPTD) system, which captures the dominant dynamics including the time delay introduced by sensor processing and converter switching. Using the graphical method, the dead time $L = 9\,\text{s}$ was determined as the interval between the step application and the first discernible change

in the output voltage, and the time constant $\tau = 39\,\mathrm{s}$ was obtained as the additional time required for the output to reach 63.2% of its final steady-state change. The static gain was calculated as the ratio of the final voltage change to the applied duty cycle step and normalized to unity ($K = 1$). The FOPTD model is therefore expressed as:

$$G(s) = \frac{K}{\tau s + 1} e^{-Ls} \tag{4}$$

where K is the plant gain, τ the time constant, and L the dead time. To verify the accuracy of the identified model, the simulated step response of this transfer function was compared with the experimental voltage response. The simulation closely matched the experimental data, capturing both the initial delay and the subsequent exponential rise; minor deviations observed in the early transient were attributed to non-linearities in the converter and battery, but the dominant dynamics were well reproduced. This qualitative agreement confirms that the FOPTD model adequately represents the plant dynamics for control design purposes, providing a reliable foundation for PID tuning and closed-loop stability analysis.

2.5.2 Closed-Loop Transfer Function

For preliminary analysis where the time delay is temporarily neglected, the simplified plant transfer function is $G_0(s) = 1/(39s + 1)$. The closed-loop transfer function for a unity-feedback system with respect to the reference input is:

$$T(s) = \frac{C(s)G_0(s)}{1 + C(s)G_0(s)} \tag{5}$$

Using the CV phase PID parameters, see Section 2.4.2 and substituting the PID controller transfer function from Equation (2) yields:

$$T(s) = \frac{0.05s^2 + 0.3s + 0.02}{39s^3 + 1.05s^2 + 0.3s + 0.02} \tag{6}$$

This third-order system's poles determine the transient behavior and stability characteristics.

2.5.3 Padé Approximation for Time Delay

To incorporate the effect of the dead time $L = 9\,\mathrm{s}$ into the analysis, a first-order Padé approximation is employed. This approximation replaces the transcendental delay term with a rational function:

$$e^{-9s} \approx \frac{1 - \frac{9}{2}s}{1 + \frac{9}{2}s} = \frac{1 - 4.5s}{1 + 4.5s} \tag{7}$$

The approximate plant transfer function then becomes:

$$G_{\text{Padé}}(s) = \frac{1}{39s + 1} \cdot \frac{1 - 4.5s}{1 + 4.5s} \tag{8}$$

The closed-loop transfer function with the Padé approximation is obtained by substituting $G_{\text{Padé}}(s)$ into Equation (5), yielding a rational transfer function that can be used for stability analysis and time-domain simulations. The introduction of a right-half-plane zero results in a non-minimum phase characteristic, which explains the undershoot observed in the step response.

These transfer functions form the foundation for evaluating the stability, transient performance, and robustness of the PID-controlled fast-charging system, enabling theoretical analysis that complements experimental validation.

3 Results

3.1 Charging Time Reduction

The experimental results demonstrate a dramatic reduction in charging time achieved by the PID-controlled CC-CV method compared to conventional constant voltage (CV) charging. As summarized in Table 2, the conventional CV method required 9 hours and 33 minutes to fully charge the 12V, 6Ah $LiFePO_4$ battery from 90% depth of discharge. In contrast, the PID-controlled CC-CV method at 0.5C (3A) completed charging in 2 hours and 1 minute, representing a 78.8% reduction in charging time. At the higher 1C rate (6A), the charging time was further reduced to just 1 hour and 7 minutes, corresponding to an 88.2% reduction compared to the CV baseline. Each protocol was repeated three times with measurement variability below 2%, and the consistency of final voltages across all methods, in 14.34V to 14.42V confirms that the battery reached full state of charge in each case, ensuring that time reductions were achieved without compromising charging completeness.

Table 2: Comparison of charging times for different methods

Charging Method	**Charging Current**	**Final Voltage**	**Time to Full Charge**	**Reduction vs. CV**
CV	Uncontrolled	14.37V	9h 33min 00s	–
CC-CV 0.5C	3 A	14.34 V	2h 01min 27s	78.8%
CC-CV 1C	6A	14.42 V	1h 07min 31s	88.2%

3.2 Voltage and Current Profiles

The voltage and current profiles during charging reveal distinct characteristics for each method, as illustrated in Figures 2–4. For conventional CV charging shown in Figure 2, the current exhibits an exponential decay from a high initial value as the battery voltage asymptotically approaches the 14.4V setpoint, resulting in a prolonged charging tail extending to 573 minutes. In contrast, the PID-controlled CC-CV method at 0.5C in Figure 3 displays a well-defined two-phase profile: during the constant current phase, the current remains stable at 3A while the voltage rises linearly to the transition threshold of 14.2V, followed by the constant voltage phase where the voltage is maintained at 14.4V while the current decays exponentially to the cutoff threshold of 0.06A. The 1C profile in Figure 4 follows the same pattern but on a compressed timescale, with the current regulated at 6A during the CC phase and a more rapid voltage rise. All profiles exhibit smooth transitions and stable regulation, confirming the effectiveness of the PID controller in maintaining setpoints and ensuring safe charging termination.

Table 3: Comparison of Step Response Characteristics

Parameter	**Exact Delay**	**Padé Approximation**	**Unit**
Rise Time	43.74	35.46	s
Settling Time	151.30	291.07	s
Overshoot	14.69	29.46	%
Undershoot	0	2.09	%

Table 4: Closed-Loop System Poles with Padé Approximation

Real Part	**Imaginary Part**	**Description**
-0.2078	0.0000	Real pole
-0.0142	0.0342	Complex conjugate pole
-0.0142	-0.0342	Complex conjugate pole

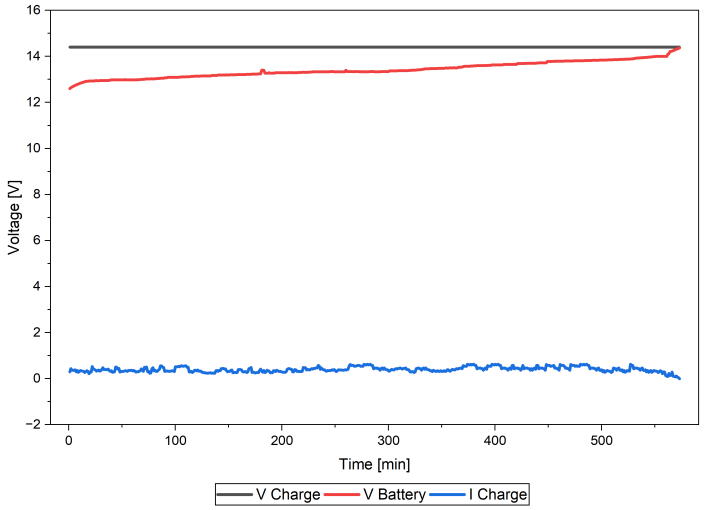

Figure 2: Constant voltage charging of a 12V 6Ah $LiFePO_4$ battery at 14.4V. Current decays slowly as voltage rises, taking 573 minutes to full charge.

3.3 Step Response and Stability Analysis

The dynamic behavior of the closed-loop system during the constant voltage phase was evaluated through step response simulation using the identified FOPTD plant model in Section 2.4.3 and the PID parameters identified in Section 2.4.2 As summarized in Table 3, the exact delay response exhibits a rise time of 43.7 seconds, settling time of 151.3 seconds, and overshoot of 14.7%, indicating a stable response suitable for battery charging applications. The Padé approximation introduces a non-minimum phase zero resulting in slight undershoot (2.1%) and higher overshoot (29.5%). The closed-loop poles obtained from the Padé approximation (Table 4)—one real pole at -0.2078 and a complex conjugate pair at $-0.0142 \pm j0.0342$—confirm system stability with a damping ratio of approximately 0.38, explaining the observed overshoot while ensuring all poles remain in the left-half plane. The consistency between simulated and experimental responses validates the modeling approach and controller tuning.

4 Discussion

The experimental and simulation results presented in this study provide comprehensive insights into the performance and dynamic behavior of the PID-controlled CC-CV fast-charging system for $LiFePO_4$ batteries [26]. This section interprets the findings in the context of existing literature, analyzes the dynamic characteristics of the control system, compares simulation and experimental results, discusses practical implications, acknowledges limitations, and outlines directions for future research.

4.1 Charging Time Reduction Analysis

The charging time reductions achieved by the PID-controlled CC-CV method (78.8% at 0.5C and 88.2% at 1C compared to conventional CV charging) represent a significant advancement over previously reported results. Khairunnisa et al. [20] reported charging times of approximately 90 minutes for a 22Ah $LiFePO_4$ battery at 0.68C, which is consistent with the 0.5C results obtained in this study when normalized for capacity. The 1C charging protocol achieves charging times comparable to fast-charging studies for other lithium-ion chemistries [21, 22], but with the added safety and longevity benefits inherent to $LiFePO_4$ technology. The dramatic improvement over CV charging is attributed to the elimination of the prolonged current decay tail characteristic of uncontrolled voltage charging, as the PID controller maintains optimal current delivery throughout the CC phase and ensures efficient

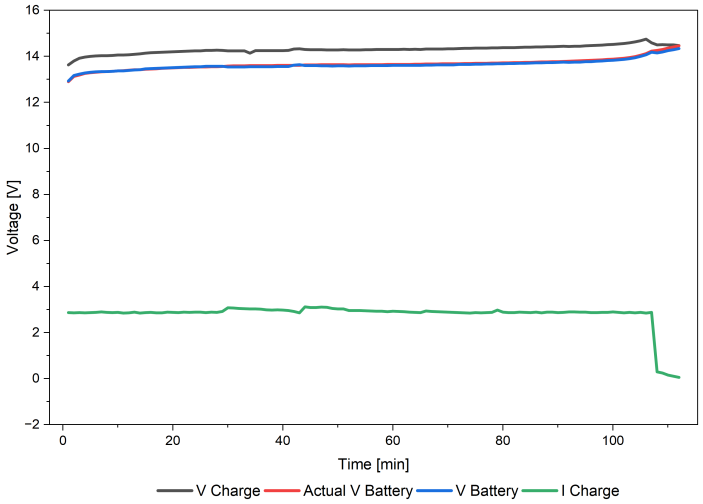

Figure 3: CC-CV fast charging of a 12V 6Ah $LiFePO_4$ battery at 0.5C rate. Constant current 3A until voltage reaches ∼14.4V, then constant voltage with current decay to 0.06A at 112 minutes

transition to CV regulation. These results position the proposed system among the fastest reported chargers for LEV-scale batteries while maintaining precise control essential for battery health.

When contextualized against alternative fast-charging strategies such as multi-stage constant current (MSCC) [23] or adaptive CC-CV based on open-circuit voltage estimation [24], our system achieves competitive charging times while offering distinct advantages in terms of implementation simplicity and cost. Unlike MSCC approaches that require complex optimization algorithms or adaptive methods that rely on accurate state-of-charge observers, our PID-controlled CC-CV charger employs a straightforward control structure that can be realized using low-cost, off-the-shelf components such as the Arduino Uno microcontroller. This simplicity translates directly into affordability, a critical factor for accelerating the adoption of light electric vehicles in developing nations where cost sensitivity is paramount. Furthermore, the modular design allows for easy replication and adaptation across different battery capacities without requiring extensive re-engineering. Thus, while the charging performance of our system aligns with more sophisticated fast-charging techniques, its primary contribution lies in democratizing access to fast-charging technology through a balance of efficiency, reliability, and cost-effectiveness.

4.2 PID Dynamic Behavior

The dynamic behavior of the PID controller during the CV phase, characterized through step response simulation, reveals a well-tuned system that balances responsiveness with stability. The closed-loop poles obtained from the Padé approximation—one real pole at -0.2078 and a complex conjugate pair at $-0.0142 \pm j0.0342$—provide valuable insight into the system's transient characteristics. The real pole dominates the fast dynamics, ensuring rapid initial response to setpoint changes, while the complex poles govern the oscillatory mode with a damping ratio of approximately 0.38, calculated from $\zeta = -\cos(\arg(p))$. This moderate damping explains the observed overshoot of 14.7%, which is acceptable for voltage regulation applications where slight overshoot does not compromise battery safety, provided it remains below the maximum voltage rating of 14.6V for $LiFePO_4$ cells. The settling time of 151.3 seconds indicates that transient disturbances are adequately rejected within a reasonable timeframe relative to the overall charging duration of 67 to 121 minutes. The derivative gain ($K_d = 0.05$) contributes critically to damping, preventing the oscillatory tendency that would otherwise arise from the interaction between the converter's inductance and the battery's capacitive behavior. The integral gain ($K_i = 0.02$), though small, ensures zero steady-state error, guaranteeing that the final voltage precisely matches the 14.4V setpoint despite parameter uncertainties or disturbances.

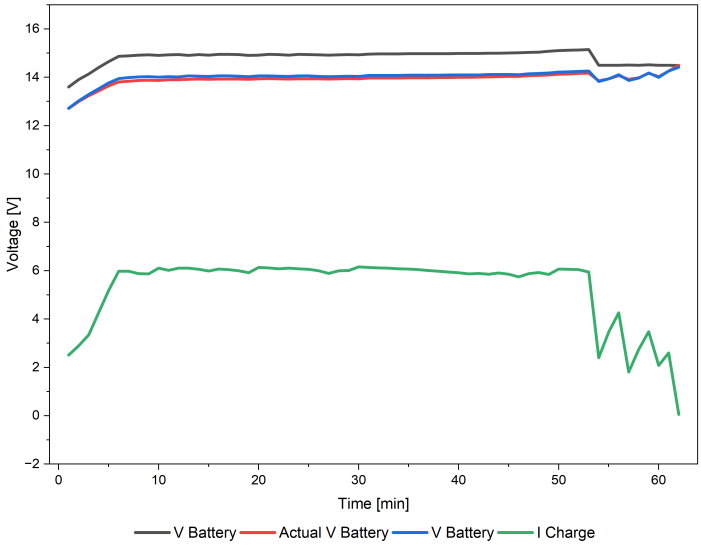

Figure 4: CC-CV fast charging profile of a 12V 6Ah $LiFePO_4$ battery at 1C rate. Constant current 6A until voltage reaches 14.2V, then constant voltage 14.4V with current decay to 0.06A at 62 minutes.

4.3 Simulation vs Experimental Comparison

The comparison between simulated step response and experimental CV phase behavior reveals excellent qualitative agreement, validating the modeling approach and controller tuning. The experimental current decay during the CV phase follows an exponential profile closely matching the simulated transient response, with both exhibiting the characteristic shape expected from a first-order system under proportional-integral control. However, quantitative differences exist: the simulated rise time of 43.7 seconds is longer than the experimentally observed time constant of the current decay, which is expected because the simulation isolates the CV phase dynamics, whereas the experimental CV phase begins with the battery already partially charged and at a higher initial state of charge. The overshoot predicted by the exact delay model (14.7%) could not be directly verified experimentally because the voltage during CV phase initiation is carefully controlled to prevent overshoot through the seamless transition algorithm. Nevertheless, the absence of voltage oscillations or instability in experimental profiles confirms that the controller maintains stability margins consistent with the analytical predictions. The Padé approximation, while introducing artificial undershoot and exaggerated overshoot, remains valuable for analytical purposes as it enables rational transfer function analysis while conservatively estimating stability margins. The identified FOPTD model adequately captures the dominant dynamics, supporting its use for control design and performance prediction.

4.4 Practical Implications

The practical implications of this research extend across multiple domains of electric vehicle technology and sustainable mobility. For light electric vehicle manufacturers, the demonstrated charging times of 1–2 hours represent a transformative improvement in user experience, potentially accelerating market adoption by addressing range anxiety and convenience concerns. The system's implementation using low-cost, commercially available components (Arduino Uno, ACS712 sensor, LM2596 converter) demonstrates that sophisticated fast-charging technology can be democratized for emerging economies, where cost sensitivity is paramount. The modular design allows straightforward adaptation to different battery capacities by scaling the C-rate setpoints, while the PID control structure can accommodate various battery chemistries through gain adjustments. From an industrial perspective, the system's compatibility with existing battery management system architectures facilitates integration into commercial charging stations and on-board chargers. Furthermore, the demonstrated 88.2% time reduction at 1C suggests potential for ultra-fast charging applications where occasional rapid top-ups

are prioritized over cycle life, such as fleet operations or emergency charging scenarios. The Indonesian government's commitment to electric vehicle adoption through Presidential Regulation No. 55/2019 [3, 4, 5] creates a favorable policy environment for deploying such technologies, aligning with national sustainability targets and supporting the development of domestic EV manufacturing capabilities.

4.5 Limitations and Future Work

Despite the promising results, this study has several limitations that warrant further investigation. Long-term cycle life testing was not conducted to assess the impact of high-rate charging on battery longevity; repeated 1C charging may accelerate degradation mechanisms such as lithium plating and solid electrolyte interface growth [10, 22], so extended cycling tests with periodic capacity measurements are necessary to quantify the trade-off between charging speed and cycle life. Thermal management was also not integrated into the current prototype; although battery surface temperature was monitored, active cooling was absent, and temperatures during 1C charging approached the upper safe limit—incorporating forced air or liquid cooling would enable sustained high-rate charging without thermal stress. The fixed transition threshold of 14.2 V may not be optimal across varying battery ages and temperatures, suggesting that adaptive transition algorithms based on real-time state-of-charge estimation [24, 25] could further optimize performance. Moreover, the PID parameters and the identified model were derived specifically for a 6 Ah $LiFePO_4$ battery; their generalizability across different capacities, manufacturers, and lithium-ion chemistries remains to be validated. Finally, integration with battery management systems for coordinated control is an essential step toward commercial deployment. Future work will address these limitations through extended cycling tests, thermal management integration, adaptive control algorithms, and validation across diverse battery types to establish the generalizability of the tuning methodology and control structure.

5 Conclusion

This study successfully developed and validated a PID-controlled constant current-constant voltage (CC-CV) fast-charging system for a 12V, 6Ah $LiFePO_4$ battery, a common energy storage unit in light electric vehicles. The experimental results demonstrate that the proposed system dramatically reduces charging time compared to conventional constant voltage charging, achieving full charge in 2 hours 1 minute at 0.5C (78.8% reduction) and 1 hour 7 minutes at 1C (88.2% reduction). The PID controller maintained excellent regulation throughout both phases, with stable current delivery during the constant-current phase and precise voltage control at 14.4V during the constant-voltage phase. The dynamic behavior was further elucidated through closed-loop transfer function modeling using a first-order plus dead time plant identified from step response data ($\tau = 39$ s, $L = 9$ s). The closed-loop poles at -0.2078 and $-0.0142 \pm j0.0342$ confirmed stability with a damping ratio of 0.38, validating the controller tuning. This research provides a validated framework for low-cost, embedded fast-charging solutions, contributing to the acceleration of LEV adoption in emerging economies. Future work will address long-term cycle life testing and thermal management integration.

Funding

This research was not funded by any organization.

Acknowledgments

The authors would like to express their profound gratitude to the Institute for Research and Community Service, Universitas Negeri Jakarta.

Author contributions

The authors contributed equally to this work. Conceptualization, R.S ; methodology, R.S, I.S and W.D; software, C.N.T; validation, I.S and R.S.; formal analysis, W.D.; investigation, R.S, I.S, C.N.T.; resources, W.D.; data curation, C.N.T.; writing—original draft preparation, R.S.; writing—review

and editing, R.S., I.S., and W.D; visualization, R.S., and C.N.T.; All authors have read and agreed to the published version of the manuscript.

Conflict of interest

The authors declare no conflict of interest.

References

[1] Mogire, E. (2026). Light Electric Vehicles and Sustainable Transport in Urban Areas: A Bibliometric Review. World Electric Vehicle Journal, 17(1), 23. https://doi.org/10.3390/wevj17010023

[2] Simo, A; Dzitac, S.; Ferestyan, L.; Dumitru, C.D.; Gligor, A. (2024). Optimizing Electric VehiclePerformance: Advances in Battery Management Systems for Enhanced Efficiency and Longevity,International Journal of Computers Communications & Control, 19(5), 6794, 2024.https://doi.org/10.15837/ijccc.2024.5.6794

[3] Maghfiroh, M .F .N.; Pandyaswargo, A .H .; Onoda, H. (2021). "Current Readiness Status of Electric Vehicles in Indonesia: Multistakeholder Perceptions" Sustainability 13, no. 23: 13177. https://doi.org/10.3390/su132313177. MDPI

[4] Damanik, N., Saraswani, R., Hakam, D. F., Mentari, D. M. (2025). A Comprehensive Analysis of the Economic Implications, Challenges, and Opportunities of Electric Vehicle Adoption in Indonesia. Energies, 18(6), 1384. https://doi.org/10.3390/en18061384

[5] Triyono, W. S.; Udisubakti, C.; Budisantoso, W.; Andhika,P. (2024). Identification of electric vehicle adoption and production factors based on an ecosystem perspective in Indonesia. Cogent Business & Management. 11. 10.1080/23311975.2024.2332497. IEEE

[6] LaMonaca, S.; Lisa. R. (2022). The state of play in electric vehicle charging services – A review of infrastructure provision, players, and policies. Renewable and Sustainable Energy Reviews. 154. 111733. 10.1016/j.rser.2021.111733. IEEE

[7] Kumar, M.; K. P. Panda.; Nayagi, R. T.; Thakur, R.; Panda, G. (2023). Comprehensive Review of Electric Vehicle Technology and Its Impacts: Detailed Investigation of Charging Infrastructure, Power Management, and Control Techniques, Applied Sciences 13, no. 15: 8919. https://doi.org/10.3390/app13158919 MDPI

[8] Suvvala, J. et al. (2024) Integration of renewable energy sources using multiport converters for ultra-fast charging stations for electric vehicles: An overview, Heliyon, vol. 10, no. 15, p. e35782, doi: 10.1016/j.heliyon.2024.e35782. SPRINGER

[9] Gulsah, Y.; Cetkin, E. (2024). Review of Cell Level Battery (Calendar and Cycling) Aging Models: Electric Vehicles, Batteries 10, no. 11: 374. https://doi.org/10.3390/batteries10110374 MDPI

[10] Li, Y. et al., Evolution of aging mechanisms and performance degradation of lithium-ion battery from moderate to severe capacity loss scenarios, Chem. Eng. J., vol. 498, p. 155588, 2024. doi: 10.1016/j.cej.2024.155588. SPRINGER

[11] Suvvala, J. et al., Integration of renewable energy sources using multiport converters for ultra-fast charging stations for electric vehicles: An overview," Heliyon, vol. 10, no. 15, p. e35782, 2024. doi: 10.1016/j.heliyon.2024.e35782. SPRINGER

[12] Zhou, W.; Yanping,Z.; Zhengjun, P.; Qiang, L. (2021). Review on the Battery Model and SOC Estimation Method, Processes 9, no. 9: 1685. https://doi.org/10.3390/pr9091685 MDPI

[13] Hoque, Md.; Hassan,M.; Khair, M.; Hajjo, A. (2023). Characteristics of Li-Ion Battery at Accelerated C-Rate with Deep Learning Method. Arabian Journal for Science and Engineering. 48. 10.1007/s13369-023-08034-x. IEEE

[14] R. Guo and W. Shen, "Recent advancements in battery state of power estimation technology: A comprehensive overview and error source analysis, J. Energy Storage, vol. 103, p. 114294, 2024. doi: 10.1016/j.est.2024.114294. SPRINGER

[15] Wang, X., Tang, Y., Li, Z. et al. (2024). Research on charging strategy based on improved particle swarm optimization PID algorithm. Complex Intell. Syst. 10, 6421–6433. https://doi.org/10.1007/s40747-024-01487-z

[16] Baicu, L. M.; Mihaela, A.; Bogdan, D. 2025. "Microcontroller-Based Platform for Lithium-Ion Battery Charging and Experimental Evaluation of Charging Strategies" Technologies 13, no. 5: 178. https://doi.org/10.3390/technologies13050178 MDPI

[17] E. Ignacio., J. Fernández., D.Giráldez., and L. Freire. (2025). "Rapid and Non-Invasive SoH Estimation of Lithium-Ion Cells via Automated EIS and EEC Models" Batteries 11, no. 9: 325. https://doi.org/10.3390/batteries11090325 MDPI

[18] B. Junting., Y. Mao., Y. Zhang., H. Xu., Y. Jiang., and Y. Yang. 2024. "Critical Review of Temperature Prediction for Lithium-Ion Batteries in Electric Vehicles" Batteries 10, no. 12: 421. https://doi.org/10.3390/batteries10120421 MDPI

[19] E. Vanem, C. B. Salucci, A. Bakdi, and Ø. Å. Alnes, "Data-driven state of health modelling—A review of state of the art and reflections on applications for maritime battery systems," J. Energy Storage, vol. 43, p. 103158, 2021. doi: 10.1016/j.est.2021.103158. IEEE

[20] Khairunnisa, K.; Mafturoh, S.M. (2023). Characteristics of LiFePo4 and Li-Ion Batteries during the Process of Charging and Discharging for Recommendation Solar Power Energy Storage. Jurnal Edukasi Elektro. 7. 53-62. 10.21831/jee.v7i1.61654.

[21] Vafaeva, K.M.; Sanjeeva, P. (2024). Comparative analysis of lithium-ion and flow batteries for advanced energy storage technologies. MATEC Web of Conferences. 392. 10.1051/matecconf/202439201176. IEEE

[22] Garita, V. V.; Heydarzadeh, M.; Dadash, A.H.; and Immonen,E. (2025) The need for aging-aware control methods in lithium-ion batteries: A review, J. Energy Storage, vol. 132, p. 117653, 2025. doi: 10.1016/j.est.2025.117653. IEEE

[23] Tahir, M. U.; Sangwongwanich, A.; Stroe, D.-I.; Blaabjerg, F. (2024) "Multi-objective optimization for multi-stage constant current charging for Li-ion batteries," J. Energy Storage, vol. 86, p. 111313. doi: 10.1016/j.est.2024.111313. SPRINGER

[24] Pavković, D.; K. Josip; Krznar, M.; C. Mihael. (2023). Adaptive Constant-Current/Constant-Voltage Charging of a Battery Cell Based on Cell Open-Circuit Voltage Estimation. World Electric Vehicle Journal. 14. Paper No. 155. 10.3390/wevj14060155. IEEE

[25] Zhong, Q., Huang, B., Ma, J., Li, H. (2013). International Journal of Smart Grid and Clean Energy Experimental study on relationship between SOC and OCV of lithium-ion batteries. International Journal of Smart Grid and Clean Energy, 3(2), 149–153. http://www.ijsgce.com/uploadfile/2015/0824/20150824072600339.pdf. SPRINGER

[26] Chen,G.-J.; Chung, W.-H. (2023). "Evaluation of Charging Methods for Lithium-Ion Batteries" Electronics 12, no. 19: 4095. https://doi.org/10.3390/electronics12194095 MDPI

[27] Montoya, G.A.; Lozano-Garzón, C.; Paternina-Arboleda, C.; Donoso, Y. (2025). A MathematicalOptimization Approach for Prioritized Services in IoT Networks for Energy-constrained Smart Cities,International Journal of Computers Communications & Control, 20(1), 6912, 2025.https://doi.org/10.15837/ijccc.2025.1.6912

Journal's webpage: http://univagora.ro/jour/index.php/ijccc/

This journal is a member of, and subscribes to the principles of,
the Committee on Publication Ethics (COPE).
https://publicationethics.org/members/international-journal-computers-communications-and-control

Cite this paper as:

Syam, R.; Djatmiko, W.; Sugihartono, I.; Trilia, C.N.; (2026). Design and Implementation of a PID-Controlled CC-CV Fast Charger for $LiFePO_4$ Batteries in Light Electric Vehicles, *International Journal of Computers Communications & Control*, 21(3), 7444, 2026.
https://doi.org/10.15837/ijccc.2026.3.7444